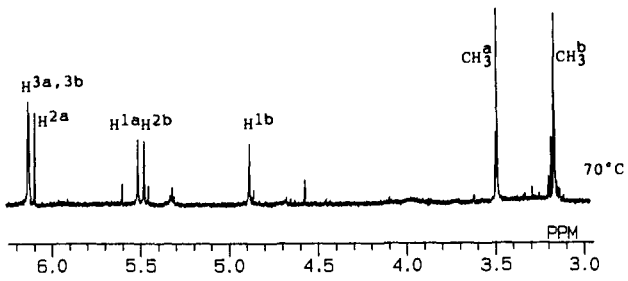

Figure 2. A 500 MHz ^{1}H NMR spectrum of **3** in toluene-d_8 at 70 °C.

diastereomeric states but enantiomeric states with equal probability ($\Delta E = 0$). The pentamer **2**, the hexamer **3**, and the tetramer **4** were isolated by gel permeation chromatography from the oligomer mixture **5**, which was prepared by the cryotachensic polymerization[16] of chloral (50.5 mmol) initiated with sodium methoxide (10.0 mmol) in toluene at 45 °C and terminated with methyl trifluoromethanesulfonate (21.2 mmol) at 10 °C. Each oligomer was purified by recrystallization from ethanol containing a small amount of chloroform.[17]

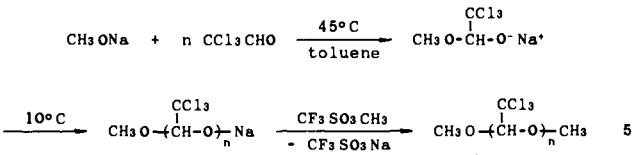

A 500 MHz ^{1}H NMR spectrum of **2** measured in toluene-d_8 at 30 °C showed signals due to methyl groups at 3.08 and 3.48 ppm and those due to methine protons at 4.84, 5.46, 5.60, and 6.03 ppm (Figure 1a);[18] these peaks are relatively broad. The sharp signal at 6.09 ppm is attributed to the methine proton of the central monomer unit of **2** (H^3). The nonequivalency of the two methyl groups and of the five acetal methine protons indicates that **2** exists in solution at 30 °C in a highly preferred conformation, probably the 4_1-helical conformation approximating the repeat gauche(−)-skew(+) ($\bar{g}s$)[19] sequences (or the repeat $\bar{5}g$ sequences). The signals, except for the signal due to H^3, became broader at 60 °C (Figure 1b), and the signals due to methyl groups coalesced at 72 °C (Figure 1c); the spectrum appeared finally as four signals with an intensity ratio of 6:2:2:1 at 105 °C (Figure 1d). Cooling the sample solution to 35 °C again completely reproduced the spectrum shown in Figure 1a. The results clearly show that the rate of helix-sense reversal becomes too fast at 72 °C for the time scale of 500 MHz NMR to distinguish the right-handed $(\bar{g}s)_5$ and left-handed $(\bar{5}g)_5$ helical states of **2**. From the spectra, the activation energy (E_a) and the rate of transition from one helical sense to the opposite sense were determined to be 16.4 kcal/mol and 3.9 s^{-1} at 20 °C, respectively. Though the coalescence temperature for the methine signals was somewhat higher (ca. 80 °C), the methine signals had a larger shift difference, and thus the E_a value estimated from the methine signals agreed with that determined from the methoxy signals (ca. 16.3 kcal/mol).

In a similar manner, the coalescence temperature for the methyl groups of the tetramer **4** was determined as 4 °C. E_a was calculated as 12.7 kcal/mol, which was 3.7 kcal/mol smaller than that for the pentamer **2**.

The hexamer **3** showed a total of seven signals with narrow line widths at 3.16, 3.48, 4.88, 5.47, 5.51, 6.09, and 6.12 (two singlets) ppm due to two methyl groups and six methine protons[18] even at 70 °C (Figure 2), indicating that the rate of the helix-sense reversal is much slower than the rate for **2**. This suggests the possibility that the symmetrical oligomers **5** over the pentamer level may be optically resolved at room temperature based entirely on conformational asymmetry.

The present results also suggest that the $(\bar{g}s)_5$ and $(\bar{5}g)_5$ states of (*R,R,R,R,R*)-(−)-**1** in solution may be distinguished by NMR spectroscopy, although the fraction of the $(\bar{5}g)_5$ state should be difficult to detect on account of the large ΔE between the two diastereomeric states. Another isotactic pentamer with a smaller ΔE (e.g., the ethoxy-initiated, methoxy-terminated pentamer) might make it possible to determine the fraction of the $(\bar{g}s)_5$ and $(\bar{5}g)_5$ states in solution by NMR spectroscopy at temperatures below the coalescence point.[20]

The purely isotactic oligomers of chloral provide unique and ideal models for the quantitative investigation of the properties of helical polymers because the oligomers have a high tendency to crystallize and very simple ^{1}H and ^{13}C NMR spectra. As far as we are aware, there is no other analogue of linear low molecular weight compounds showing such slow interconversion between enantiomeric helical states.

(16) (a) Vogl, O.; Miller, H. C.; Sharkey, W. H. *Macromolecules* **1972**, *5*, 658. (b) Zhang, J.; Jaycox, G. D.; Vogl, O. *Polymer* **1988**, *29*, 707. (c) Hatada, K.; Ute, K.; Nakano, T.; Vass, F.; Vogl, O. *Makromol. Chem.* **1989**, *190*, 2217.

(17) The crystals of **2** and **4** started to decompose at 182 and 178 °C, respectively, before melting.

(18) The assignment of the ^{1}H NMR signals was unambiguously made together with that of ^{13}C NMR signals by the procedure (the ^{13}C NMR selective ^{1}H-decoupling method) described in the previous papers.[11b,16c] Dihedral angle dependence of the $^3J_{COCH}$ coupling constants suggested that the backbone conformations of **1** and **2** were essentially identical.

(19) For the notations of the internal rotation angle, see: Tadokoro, H. In *Structure of Crystalline Polymers*; John Wiley & Sons: New York, 1979; p 14.

(20) Very recently, this was confirmed for the ethoxy-initiated, methoxy-terminated, purely isotactic pentamer of chloral. The ratio of the two helical states was 17:8 in chloroform-*d* at 0 °C: Ute, K.; Kashimoto, H.; Hatada, K.; Vogl, O., manuscript in preparation.

Design and Synthesis of a Knot from Single-Stranded DNA

John E. Mueller,† Shou Ming Du, and Nadrian C. Seeman*

Department of Chemistry, New York University
New York, New York 10003

Received April 22, 1991

The possibility that polymers can be knotted was pointed out by Frisch and Wasserman 30 years ago.[1] Numerous investigators have attempted to form knots in small-molecule systems;[2,3] recently, a synthetic knot has been reported.[4,5] Large, double-stranded DNA molecules are knotted by recombination enzymes using double-strand breaks,[6-9] whereas large single-stranded DNA molecules can be knotted by type I topoisomerases.[10] The plectonemic structure of the nucleic acid double helix[11] offers a convenient way for controlling the braiding of one part of a molecule about another part. This feature has recently been used to construct a multiply catenated cubelike DNA structure, in which every nucleotide is designed to be paired.[12] Likewise, single-stranded DNA containing complementary regions interspersed between relatively unstructured oligo-dT tracts is an ideal substance for the design and synthesis of knots. In contrast to previous approaches,[2,4] the braiding part of the molecular backbone

† Permanent address: Department of Biological Sciences, SUNY/Albany, Albany, NY 12222.

(1) Frisch, H. L.; Wasserman, E. *J. Am. Chem. Soc.* **1961**, *83*, 3789-3795.
(2) Walba, D. M. *Tetrahedron* **1985**, *41*, 3161-3212.
(3) Sauvage, J.-P. *Acc. Chem. Res.* **1990**, *23*, 319-327.
(4) Dietrich-Buchecker, C. O.; Sauvage, J.-P. *Angew. Chem., Int. Ed. Engl.* **1989**, *28*, 189-192.
(5) Dietrich-Buchecker, C. O.; Guilhem, J.; Pascard, C.; Sauvage, J.-P. *Angew. Chem., Int. Ed. Engl.* **1990**, *29*, 556-557.
(6) Mizuuchi, K.; Fisher, L. M.; O'Dea, M. H.; Gellert, M. *Proc. Natl. Acad. Sci. U.S.A.* **1980**, *77*, 1847-1851.
(7) Wasserman, S. A.; Cozzarelli, N. R. *Science* **1986**, *232*, 951-960.
(8) Griffith, J. D.; Nash, H. A. *Proc. Natl. Acad. Sci. U.S.A.* **1985**, *82*, 3124-3128.
(9) Liu, L. F.; Liu, C.-C.; Alberts, B. M. *Cell* **1980**, *19*, 697-707.
(10) Liu, L. F.; Depew, R. E.; Wang, J. C. *J. Mol. Biol.* **1976**, *106*, 439-452.
(11) Watson, J. D.; Crick, F. H. C. *Nature* **1953**, *171*, 737-738.
(12) Chen, J.; Seeman, N. C. *Nature* **1991**, *350*, 631-633.

0002-7863/91/1513-6306$02.50/0

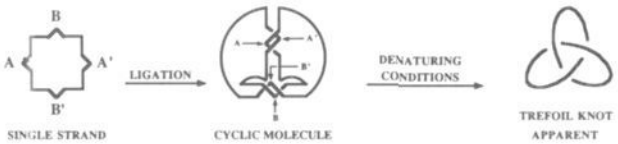

Figure 1. *Synthetic scheme for the single-stranded DNA knot.* The starting material is illustrated on the far left: **A** (ACTGGACCTCT), **B** (CGTAGCCGCAT), **A′**, and **B′** refer to the regions that are expected to pair by Watson–Crick hydrogen bonding. Each side of the square figure shown corresponds to a quarter of the molecule. The projections represent the regions that will pair according to the letter codes; they are flanked by the oligo-T linkers. The arrowhead within the **A** projection represents the 3′ end of the strand. The central portion of the figure is a disorted structure showing the interlinking of the ligated strand. The double-helical linking is concentrated in one portion of each helical domain.[19] Both helices are viewed from the minor groove side at the middle. The oligo-T linkers are represented with distorted scales by the curved portions of the strand. The vertical helix is further from the viewer than the horizontal one, as indicated by its lighter lines. The trefoil structure is drawn (far right) in an idealized fashion. The handedness of the trefoil is appropriate for right-handed double-helical DNA.

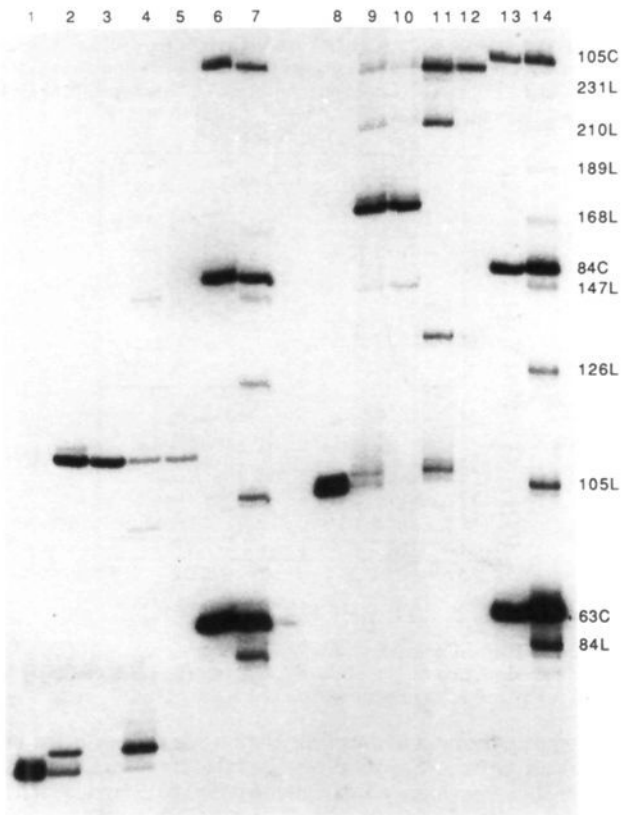

Figure 2. *Synthesis of the knot.* This is an autoradiogram of a denaturing 10% polyacrylamide gel containing the 72-mer and 104-mer species examined. The DNA has been synthesized and deprotected by routine phosphoramidite methods[20] and has been phosphorylated and ligated as described earlier.[21] The material in lanes 1–5 is a 72-mer and the material in lanes 8–12 is a 104-mer. Lanes 7 and 14 contain linear ("L") and circular ("C") markers generated by ligating a three-arm DNA branched junction containing 21 nucleotide pairs between vertices.[22] Lanes 6 and 13 contain the same material treated with exonuclease III to produce circular markers.[22] Lanes 1 and 8 contain linear molecules that have been phosphorylated but not treated with ligase. Lanes 2 and 9 contain material that has been treated with ligase, while lanes 3 and 10 contain ligated material that has been treated with exonuclease III. The material in lanes 4 and 11 is linear DNA that has been ligated in the presence of a circle-promoting complement (10 and 15 nucleotide overlap on respective ends of the nick), and the result of treating this material with exonuclease III is shown in lanes 5 and 12. Note that a new species is seen to run faster than the circle in lane 10, but not in lane 3. This appears to be the target knot. A very faint band is visible running faster than this material and may correspond to a 5_2 knot.

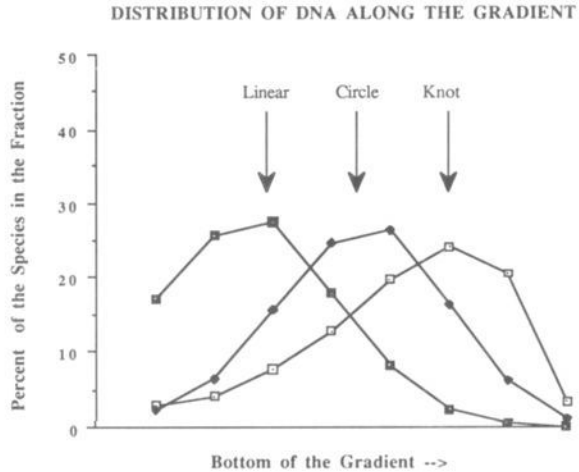

Figure 3. *Sedimentation analysis of linear, circular, and knotted 104-mer DNA molecules.* Samples of each species have been ^{32}P labeled, mixed together, layered on a 5–20% sucrose gradient, pH 12.1, and spun at 45 000 rpm for 24 h in a SW60 swinging-bucket rotor. Twenty-eight fractions of the 4-mL solution have been collected, applied to a denaturing polyacrylamide gel, electrophoresed, quantitated on a Betagen Betascope 603 blot analyzer, and normalized to 100%. The 8 fractions shown correspond to the 11th through 18th fractions from the top of the gradient; these are the only fractions containing detectable material. The knot is clearly the most rapidly sedimenting species present.

is chemically identical with the nonbraiding part. A trefoil knot can be modeled from 2 full turns of double-helical DNA, using an A–B–A′–B′ pairing motif.[13] Here we report construction of a molecule like this and demonstrate that its electrophoretic and sedimentation properties differ from those of a circle with same sequence.

We have designed a single-stranded sequence containing four pairwise-complementary 11-mer sequences (Figure 1). Each pairing region is separated by a dT_n spacer, where n equals 7 or 15. Sequence **A** complements **A′** and **B** complements **B′**. The 5′ and 3′ ends of the synthetic molecule fall between the 8th and 9th nucleotide of the **A** segment, producing a nick that can be sealed by T4 DNA ligase. Regardless of its native structure, the fundamental topology of the molecule is expected to be a trefoil knot; therefore, we have characterized the ligation products under denaturing conditions.

The results of the ligation experiment are illustrated in Figure 2. Lanes 1–5 show the ligation of a molecule containing 72 nucleotides ($n = 7$), and lanes 8–12 illustrate the same experiment with a molecule containing 104 nucleotides ($n = 15$). Lanes 3 and 10 contain ligated material that has been digested with exonuclease III to remove linear molecules. Both lanes 3 and 10 contain some material that migrates similarly to circular markers of the appropriate length (lanes 5 and 12). No material larger than the circle survives exonuclease digestion, suggesting that double-length circles and catenanes are not formed.[14] Only lane 10 contains an additional exonuclease III-resistant species, one that migrates faster than the circle. Under appropriate conditions, double-stranded DNA knots of greater complexity are known to migrate more rapidly than DNA circles of the same length.[15,16] The 72-residue molecule does not form a knot, indicating that the minimum length for n lies somewhere between 7 and 15.

The denaturing Ferguson plot[17] of the new species shows 10% greater slope than the circle, intersecting it at 17% polyacrylamide (data not shown). This experiment establishes the uniqueness of the two molecules, but it also implies that the greater mobility

(13) Seeman, N. C. *J. Biomol. Struct. Dyn.* **1988**, *5*, 997–1004.
(14) Krasnow, M. A.; Cozzarelli, N. R. *J. Biol. Chem.* **1982**, *257*, 2687–2693.
(15) Dean, F. B.; Stasiak, A.; Kollier, T.; Cozzarelli, N. R. *J. Biol. Chem.* **1984**, *260*, 4975–4983.
(16) White, J. H.; Millett, K. C.; Cozzarelli, N. R. *J. Mol. Biol.* **1987**, *197*, 585–603.
(17) Rodbard, D.; Chrambach, A. *Anal. Biochem.* **1971**, *40*, 95–134.

of the putative knot is inconclusive proof of its identity, because relative mobility is a function of gel concentration. Sedimentation velocity offers a direct physical measurement of the relative compactness of a molecule. Figure 3 shows the results of a sedimentation experiment illustrating that the new species sediments faster than the circle of the same sequence under denaturing conditions.[10]

The knot molecule formed here is the first of a series of knots that appear constructable from synthetic single-stranded DNA or RNA. Nucleic acid knots have the virtue that it is easy to make circular structures from the same molecule, thus providing a baseline structure for determining the physical properties[18] of these unusual molecular topologies. The A-B-A′-B′ motif used here will result in more complex knots if longer double-helical segments are used; more complex motifs and other strategies will generate additional knots.

Acknowledgment. This research has been supported by Grant GM-29554 from the NIH. We are grateful to Dr. Nicholas Cozzarelli for providing us with a copy of the program KNOTTER by John Jenkins. We thank Drs. Stuart Fischer and Richard Cunningham for very valuable discussions and for helping with the sedimentation experiment. Dr. Reid Johnson has also provided helpful advice for this study. We are indebted to the W. M. Keck Foundation for their support of biomolecular imaging at NYU.

(18) Moffat, H. K. *Nature* **1990**, *347*, 367-369.
(19) Chen, J.-H.; Kallenbach, N. R.; Seeman, N. C. *J. Am. Chem. Soc.* **1989**, *111*, 6402-6407.
(20) Caruthers, M. H. In *Chemical and Enzymatic Synthesis of Gene Fragments*; Gassen, H. G., Lang, A., Eds.; Verlag Chemie: Weinheim, 1982; pp 71-79.
(21) Mueller, J. E.; Kemper, B.; Cunningham, R. P.; Kallenbach, N. R.; Seeman, N. C. *Proc. Natl. Acad. Sci. U.S.A.* **1988**, *85*, 9441-9445.
(22) Ma, R. I.; Kallenbach, N. R.; Sheardy, R. D.; Petrillo, M. L.; Seeman, N. C. *Nucl. Acids Res.* **1986**, *14*, 9745-9753.

Alkyl Iodide Decomposition on Copper Surfaces: α-Elimination and β-Hydride Elimination from Adsorbed Alkyls

Cynthia J. Jenks, Chao-Ming Chiang, and Brian E. Bent*

Columbia University, Department of Chemistry
New York, New York 10027

Received February 12, 1990
Revised Manuscript Received May 20, 1991

While many studies have addressed carbon-hydrogen bond activation at the α and β positions in metal-alkyl compounds,[1-3] little is known about the analogous processes on transition-metal surfaces.[4] We report here mechanistic studies of C-H bond activation in alkyls generated on a Cu(110) single crystal surface by dissociative adsorption of alkyl iodides. Our results enable us to compare the rates of β-hydride elimination and α-elimination on copper surfaces. Specifically, we find that the rate of β-hydride elimination from linear alkyls is over 6 orders of magnitude faster than the rate of α-elimination from adsorbed methyl groups.

The experiments were performed in two ultrahigh vacuum systems equipped with low-energy electron diffraction (LEED), Auger electron spectroscopy (AES), quadrupole mass spectrometry, and high-resolution electron energy loss spectroscopy (HREELS).[5] Using these techniques; we have found that, analogous to other metal surfaces,[4,6-9] alkyl iodides thermally dissociate on copper surfaces below 200 K to form alkyl groups

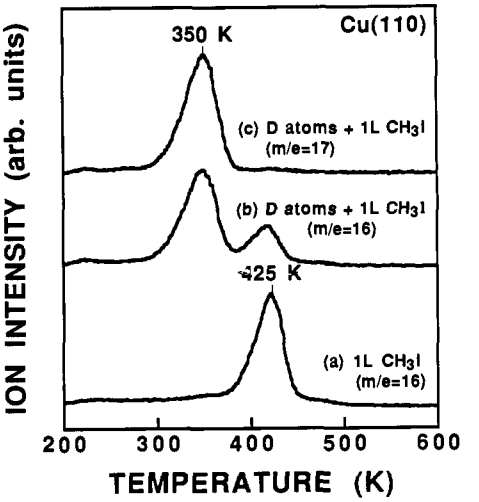

Figure 1. Thermal evolution of methane and partly deuterated methane after adsorption of CH_3I on Cu(110) at 110 K with and without coadsorbed deuterium atoms: (a) desorption of m/e = 16 (CH_4^+) after adsorption of 1.0 L of CH_3I; (b and c) desorption of m/e = 16 (CH_4^+, CH_2D^+) and m/e = 17 (CH_3D^+) respectively after preadsorption of deuterium atoms generated using a hot tungsten filament followed by 1.0 L of CH_3I. The D/CH_3I ratio on the surface in these experiments is 4. The heating rate is 2.5 K/s.

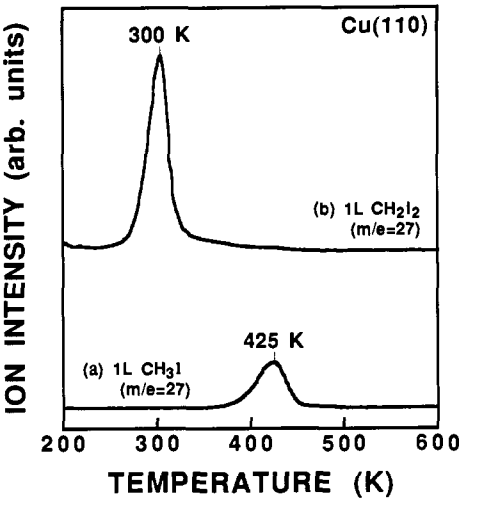

Figure 2. Thermal evolution of ethylene [monitoring m/e = 27 ($C_2H_3^+$)] after the adsorption of (a) 1.0 L of CH_3I and (b) 1.0 L of CH_2I_2 on Cu(110) at 110 K. The heating rate is 2.5 K/s.

(1) (a) Burk, M. J.; McGrath, M. P.; Crabtree, R. H. *J. Am. Chem. Soc.* **1988**, *110*, 620. (b) Fellmann, J. D.; Schrock, R. R.; Traficante, D. D. *Organometallics* **1982**, *1*, 481-484. (c) Shilov, A. E.; Shteinman, A. A. *Coord. Chem. Rev.* **1977**, *24*, 97-143. (d) Cree-Uchiyama, M.; Shapley, J. R.; St. George, G. M. *J. Am. Chem. Soc.* **1986**, *108*, 1316-1317.
(2) Parkin, G.; Bunel, E.; Burger, B. J.; Trimmer, M. S.; Van Asselt, A.; Bercaw, J. E. *J. Mol. Catal.* **1987**, *41*, 21-39.
(3) For more general references, see: (a) Collman, J. P.; Hegedus, L. S.; Norton, J. R.; Finke, R. G. *Principles and Applications of Organotransition Metal Chemistry*; University Science Books: Mill Valley, CA, 1980; Chapter 6. (b) Kochi, J. K. *Organometallic Mechanisms and Catalysis*; Academic Press, Inc.: New York, NY, 1978; Chapter 12. (c) Davidson, P. J.; Lappert, M. F.; Pearce, R. *Chem. Rev.* **1976**, *76*, 219-242. (d) Schrock, R. R.; Parshall, G. W. *Chem. Rev.* **1976**, *76*, 243-268.
(4) Recent studies have documented β-hydride elimination by alkyl groups bound to aluminum and platinum: (a) Bent, B. E.; Nuzzo, R. G.; Dubois, L. H. *J. Am. Chem. Soc.* **1989**, *111*, 1634-1644. (b) Bent, B. E.; Nuzzo, R. G.; Zegarski, B. R.; Dubois, L. H. *J. Am. Chem. Soc.* **1991**, *113*, 1137-1142. (c) Zaera, F. *J. Am. Chem. Soc.* **1989**, *111*, 8744-8745. (d) Zaera, F. *Surf. Sci.* **1989**, *219*, 453-466. (e) Lloyd, K. G.; Campion, A.; White, J. M. *Catal. Lett.* **1989**, *2*, 105-112. (f) Zaera, F. *J. Phys. Chem.* **1990**, *94*, 8350-8355.
(5) (a) Chiang, C.-M.; Wentzlaff, T.; Bent, B. E., submitted to *J. Phys. Chem.* (b) Jenks, C. J.; Smoliar, L.; Tsang, S.; Bent, B. E., to be submitted to *Surf. Sci.* (c) Lin, J.-L.; Bent, B. E., to be submitted to *J. Chem. Phys.*
(6) (a) Zhou, X.-L.; Solymosi, F.; Blass, P. M.; Cannon, K. C.; White, J. M. *Surf. Sci.* **1989**, *219*, 294-316. (b) Zhou, X.-L.; White, J. M. *Catal. Lett.* **1989**, *2*, 375-384.
(7) (a) Zhou, X.-L.; White, J. M. *Chem. Phys. Lett.* **1987**, *142*, 376-380. (b) Zhou, X.-L.; White, J. M. *Surf. Sci.* **1988**, *194*, 438-456.
(8) Henderson, M. A.; Mitchell, G. E.; White, J. M. *Surf. Sci.* **1987**, *184*, L325-L331.
(9) Roop, B.; Zhou, Y.; Liu, Z.-M.; Henderson, M. A.; Lloyd, K. G.; Campion, A.; White, J. M. *J. Vac. Sci. Technol. A* **1989**, *7*, 2121-2124.

0002-7863/91/1513-6308$02.50/0